Swansea University
Prifysgol Abertawe

Quantifying functional group abundances of intertidal canopy-forming brown macroalgae: combining unmanned aerial vehicle and satellite imagery with machine learning

Joshua Mutter

Swansea University

Submitted to Swansea University in fulfilment of the requirements for the Degree of Master of Research

April 2024

Abstract

Canopy-forming brown macroalgae provide structural support for a diverse range of rocky shore organisms, altering rocky coastline into vibrant coastal macroalgal forests. Intertidal macroalgae provide a range of ecosystem services, and macroalgal forest cover is considered an essential ocean variable for monitoring the anthropogenic degradation of coastal ecosystems. Advances in remote sensing techniques, including machine learning and brown algae index (BAI), could upscale efforts to remotely map intertidal macroalgal forests using multispectral satellite imagery. However, previous machine learning application is limited to higher resolution images from small aircraft, whereas BAI regression techniques lack validation on heterogeneous or diverse intertidal forests and are limited to broad taxonomic groups containing multiple spectrally variable species. Random Forests classifiers were trained using unmanned aerial vehicle (UAV) data from four shores around the UK. I used this to predict functional group cover based on multispectral images from the European Space Agency's Sentinel-2 satellite both i) within the original training shores, and ii) two new sites independent of model training. Total cover estimates were compared to those from previously employed BAI regression models, and re-parameterised BAI regression models using data from the four training shores containing greater heterogeneity and diversity. Random forest models accurately predicted functional group cover during within-set cross-validation but require the incorporation of intra-species variation in reflectivity to predict group cover on novel shores containing different environmental conditions and species traits. BAI regression models provided more robust estimates of total brown macroalgal cover when fitted to data that reflects the natural range heterogeneity and diversity present in intertidal macroalgae habitats. Caution is advised when applying a single BAI regression model as factors that impact near-infra-red or green reflectance can weaken predictability, such as variations in species reflectivity. Nevertheless, results revealed that multispectral satellite imagery can upscale the mapping of intertidal macroalgal coverage around heterogeneous UK shores, improving estimations of ecosystem services and monitoring of anthropogenic degradation.

Declarations

This work has not previously been accepted in substance for any degree and is not being concurrently submitted in candidature for any degree.

Signed.................... ████████████ ....

Date........................ 14/2/2024 ....

This thesis is the result of my own investigations, except where otherwise stated. Other sources are acknowledged by footnotes giving explicit references.   A bibliography is appended.

Signed............. ████████████████

Date.................. 14/2/2024

I hereby give consent for my thesis, if accepted, to be available for electronic sharing

Signed........................... ████████████ ....

Date........................ 14/2/2024 ....

The University's ethical procedures have been followed and, where appropriate, that ethical approval has been granted.

Signed................. ████████████ ....

Date.................... 14/2/2024 ....

3

Statement of Expenditure

Category	Description	Cost
Fieldwork	Car hire and accommodation	£2000.00

Statement of Contribution

Contributor role	Contributor
Conceptualisation	JG
Data curation	TF, JM
Formal analysis	JM
Funding acquisition	JG
Investigation	TF, JM
Methodology	TF, JM
Project administration	JG
Resources	JG
Supervision	JG, TF
Validation	TF, JM
Visualisation	JM
Writing – Original Draft Preparation	JM
Writing – Review & Editing	JG, TF, JM

JG – Dr John Griffin

TF – Dr Tom Fairchild

JM – Joshua Mutter

Copy of ethics approval

Approval Date: 21/03/2024

Research Ethics Approval Number: 1 2024 9470 8401

Thank you for completing a research ethics application for ethical approval and submitting the required documentation via the online platform.

Project Title	Quantifying functional group abundances of intertidal canopy-forming brown macroalgal: combining UAV and satellite imagery with machine learning
Applicant name	MR JOSHUA MUTTER
Submitted by	MR JOSHUA MUTTER /
Full application form link	https://swansea.forms.ethicalreviewmanager.com/Project/Index/11502

The Science and Engineering ethics committee has approved the ethics application, subject to the conditions outlined below:

Approval conditions

1. The approval is based on the information given within the application and the work will be conducted in line with this. It is the responsibility of the applicant to ensure all relevant external and internal regulations, policies, and legislations are met.
2. This project may be subject to periodic review by the committee. The approval may be suspended or revoked at any time if there has been a breach of conditions.
3. Any substantial amendments to the approved proposal will be submitted to the ethics committee prior to implementing any such changes.

Specific conditions in respect of this application:

The application has been classified as Low Risk to the University.

No additional conditions.

Statement of compliance

The Committee is constituted in accordance with the Governance Arrangements for Research Ethics Committees. It complies with the guidelines of UKRI and the concordat to support Research Integrity.

Science and Engineering Research and Ethics Chair

Swansea University.

If you have any queries regarding this notification, then please contact your research ethics administrator for the faculty.

- For Science and Engineering contact FSE-Ethics@swansea.ac.uk
- For Medicine, Health and Life Science contact FMHLS-Ethics@swansea.ac.uk
- For Humanities and Social Sciences contact FHSS-Ethics@swansea.ac.uk

Copy of risk assessment

Risk Assessment	
Quantifying functional group abundances of intertidal canopy-forming brown macroalgal: combining UAV and satellite imagery with machine learning	

College/PSU	Bioscience	Assessment Date	04/02/23
Location	Rocky Shores	Assessor	Joshua Mutter
Activity	Rocky Shore Fieldwork	Review Date (if applicable)	N/A
Associated documents	●	●	

Part 1: Risk Assessment

What are the hazards?	Who might be harmed?	How could they be harmed?	What are you already doing?	Do you need to do anything else to manage this risk?	Action by whom?	Action by when?	Done Yes/ No
Uneven/ slippery surface	All	Fall, twist ankle, other physical injuries	Due diligence, wear appropriate footwear/clothing, first aid kit and radio on hand, no lone working, first aid training, PPE	No	N/A	N/A	N/A
Tide/waves	All	Isolated, swept away, drown	Due diligence, tide tables, lifeguard and first aid training	No	N/A	N/A	N/A
Adverse weather	All	Wind chill, hypothermia, slip/fall	Appropriate outdoor clothing	No	N/A	N/A	N/A
Isolation/ Poor access	All	Other hazards enhanced by this	Ensure that someone knows the location and return time. Buddy system to always be used. Protocol to contact emergency services after a predetermined time.	No	N/A	N/A	N/A
COVID-19 symptoms	All	Contracting severe illness	Symptomatic person isolated beforehand and follow NHS advice. Hands, face space.	No	N/A	N/A	N/A
Conflict during aircraft use	Other air users, wildlife	Airprox incident, collision, aircraft damage	Conduct pre-flight survey of area to identify flight restrictions or advisories, and check for transient restrictions using NATS and drone. map platforms. This includes identifying any aerodrome operations area, near military facilities or other sensitive sites where flight is prohibited. Stay below 400ft (120m) This reduces the likelihood of a conflict with manned aircraft. Maintain a visual and audible awareness of any approaching aircraft (and returning to home if necessary) - via both the designated pilot and observer	No	N/A	N/A	N/A

Screenshot of risk assessment approval

Science fieldwork risk assessment (UG/PGT/PGR)

You must not carry out fieldwork until this risk assessment has been approved by your Supervisor. See the Fieldwork Risk Assessment Guidance document to complete this form.

Risk Assessment Outcome:

Risk Rating: Moderate/High risk   **Submitted Date:** 20 Mar 2024

Approved Date: 21 Mar 2024   **Approved by:** John Griffin

Student Details

Student Number: ▌▌▌▌   **Project Supervisor:** Dr John Griffin

Course: Biosciences Masters by Research Full-time   **Level:** 7

Assessor:	Joshua Mutter	Assessment Date:	21/03/2024
Contact Number:	▌▌▌▌	No. of Participants:	1
Next of Kin:	Jill Hopcraft	Next of Kin Contact Number:	▌▌▌▌

Name of field assistant(s) – Lone working is only permitted in exceptional circumstances, with the agreement of your

Contents

Acknowledgements

List of Figures and Tables

List of Abbreviations

BAI   Brown Algae Index

UAV   Unmanned Aerial Vehicle

Introduction

Coastal habitats and macroalgal forests

Canopy-forming brown macroalgae engineer barren rocky coastlines into complex three-dimensional habitats, where large brown species provide shelter to a varied community of benthic fauna and flora (Lamy et al., 2020; Metzger et al., 2019). Environmental conditions vary greatly within the relatively small areas of intertidal zones compared to terrestrial or subtidal aquatic habitats (Underwood, 2000). For instance, variation in exposure along local coastlines and desiccation stress within individual shores creates pronounced zonation of macroalgal species (Underwood & Jernakoff, 1984), in addition to biotic factors including interspecific competition and grazing pressure that can limit spatial extents further impacting zonation patterns (Hawkins et al., 2020; Underwood & Jernakoff, 1984). The pronounced zonation patterns within relatively small areas provide ideal habitats to evaluate the effect of abiotic environmental variables and biotic interactions on community structuring (Hawkins et al., 2020). In the North Atlantic, common canopy-forming macroalgae range from fucoid rockweeds including *Ascophyllum nodosum* and *Fucus* species to larger kelp species such as *Laminaria digitata* and *Saccharina latissima* (Yesson et al., 2015). This diversity of macroalgal species likely contributes to the wide array of ecosystem services they provide, including biodiversity enhancement (Lamy et al., 2020; Metzger et al., 2019), coastal defence, nursery habitats, and carbon sequestration, although this last service remains poorly understood and previously overlooked due to the lack of *in-situ* sedimentary carbon storage (Bayley et al., 2021; Edgar & Moore, 1986; Krumhansl & Scheibling, 2011; Lewis et al., 2023; Teagle et al., 2017; Thornber et al., 2016). Moreover, certain macroalgae can indicate coastline health (D'Archino & Piazzi, 2021; Juanes et al., 2008; Pinedo et al., 2007), and others are harvested for beneficial compounds like alginates, which can provide economic support for local populations in addition to fishery supplementation (Bertocci et al., 2015; Edgar & Moore, 1986; Greenhill et al., 2021; Vondolia et al., 2020; Wing et al., 2022).

Threats to macroalgae forests

Coastal habitats including macroalgal forests are under threat from loss of available habitat due to factors such as coastal development, anthropogenic pollution (Orlando-Bonaca et al., 2021; Yesson et al., 2015), and climate change (Hawkins et al., 2008; Norderhaug et al., 2020). Macroalgal forest cover is proposed to be an essential ocean variable that can be used to evaluate the impact of anthropogenic threats like climate change on coastal habitats (Miloslavich et al., 2018; Yesson et al., 2015). Consequently, the ability to remotely estimate macroalgal cover would improve the efficiency of recording anthropogenic impacts on coastal habitats and enable effective mitigation or management (Brodie et al., 2018; Lewis et al., 2023; Rossiter et al., 2020). Furthermore, accurate

mapping of macroalgal species could aid the assessment of biodiversity's role in maintaining functionality and service provision of ecological communities over varying environmental contexts, especially over large region-sized scales (Schrofner-Brunner et al., 2023; Weiskopf et al., 2022). Yet, while *in situ*, manual, sampling of macroalgal habitats is done in developed and easily accessible locations, developing spatially explicit remote sensing techniques could expand application and reduce the reliance on extensive, costly, and time-prohibitive field surveys. Additionally, using open-access satellite imagery further increases the scope of application, compared to aerial surveys or hyperspectral imagery, which can be limited by the cost and workload associated with capturing larger areas. Moreover, researchers can capitalize on time series of satellite imagery, with examples such as Sentinel and Landsat capturing images continuously since 2015 and 1972 respectively.

Remote sensing application in coastal habitats

Historically, quantitative estimates of macroalgal extents have been predominantly based on labour-intensive field surveys or broad-scale mapping of forests from aerial photographic surveys (Brodie et al., 2018; Burrows, 2012). Spatial extents are then related to environmental conditions that govern species distribution models. However, the accuracy of species distribution models can be limited by the low resolution of environmental data. Furthermore, a lack of understanding of the rules governing ecological assembly at finer-scale variations of environmental gradients, such as substrate rugosity, can reduce the accuracy of species distribution models (Dudley & D'Antonio, 1991; Muth, 2012; Schrofner-Brunner et al., 2023; Underwood & Jernakoff, 1984). As an alternative or complement to modelling distributions based on limited data, researchers can use remote sensing to directly map habitat coverage over large scales. Remote sensing techniques have been successfully applied to tropical habitats such as coral reefs, seagrass meadows, and mangrove forests, as well as temperate subtidal kelp forests and intertidal fucoid assemblages (Finger et al., 2021; Hamilton et al., 2020; Purkis, 2018; Veettil et al., 2020; L. Wang et al., 2019). Remote sensing techniques can identify spectral characteristics between regions of interest due to differences in reflectance patterns over different electromagnetic wavelengths (Brodie et al., 2018; DeFries & Chan, 2000; Lewis et al., 2023). Due to their bidaily tidal exposure, intertidal macroalgal forests present model target habitats for the application of remote sensing techniques, because of reduced interference from deeper water on algae reflectivity (Brodie et al., 2018; Malthus & George, 1997). However, previous mapping of macroalgae has been predominantly restricted to broad habitat types or vegetation indices targeted to a single broad group of interest (Kotta et al., 2018; Lewis et al., 2023; Rossiter et al., 2020).

Vegetation indices and macroalgae

Vegetation indices can target broad vegetation types within ecosystems such as forests, grasslands, and coastal habitats (Hu, 2009; Lewis et al., 2023; Mora-Soto et al., 2020; Siddiqui & Zaidi, 2023). Previous studies have established vegetation indices specific to macroalgae and have been employed to estimate cover. These indices include the floating algal index, seaweed enhancing index, and brown algae index (BAI) (Hu, 2009; Lewis et al., 2023; Mora-Soto et al., 2020; Siddiqui et al., 2019). Some of these indices can differentiate between broad habitat classes within macroalgae forests (Lewis et al., 2023; Mora-Soto et al., 2020), while others use specific thresholds within more generalised vegetation indices, such as the normalised difference vegetation index (NDVI; (Cui et al., 2018), and the enhanced vegetation index (EVI; (Siddiqui et al., 2019). The spectral resolution of the imagery used significantly impacts the performance of vegetation indices and image resolution is mainly dependent on the altitude of the sensor during image capture (Kotta et al., 2018; Lewis et al., 2023; Rossiter et al., 2020). Unmanned aerial vehicles (UAV) provide high-resolution imagery of limited areas due to restrictions in battery life, access, and weather conditions. On the other hand, satellites like the European Space Agency's Sentinel-2 provide open-access satellite imagery with a resolution of approximately 6-10m and a resample time of 2-3 days (European Space Agency, 2015; Phiri et al., 2020) However, availability is limited by cloud cover, and coordination with low tide for intertidal areas. Greater resolution images are available, such as DigitalGlobe's WorldView-3 satellite supplying multispectral imagery with 1.24m resolution (DigitalGlobe, 2014). However, commercial imagery such as this is prohibitively costly, especially when covering large areas or along extensive coastlines.

Combining UAV and satellite imagery to improve cover estimates

By combining high-resolution UAV cover observations with multispectral satellite imagery, research has improved the mapping of macroalgal forests using satellite imagery (Duarte et al., 2022; Kotta et al., 2018; Lewis et al., 2023). The utility of UAVs in this context is that they allow accurate quantification of macroalgal cover on scales that are impractical to manually survey. Cui et al. (2018) applied statistical regression models combining high-resolution cover predictions with those from satellite imagery to improve the detection of floating green algal blooms from satellite images. Later, this technique was applied to intertidal brown canopy-forming macroalgae. Lewis *et al.* (2023) introduced the brown algae index (BAI), which effectively identified canopy-forming brown macroalgae from UAV imagery. Using polynomial regression models they predicted brown canopy-forming macroalgal cover using BAI values from Sentinal-2 imagery. The use of statistical regression models has enabled accurate predictions of brown canopy-forming macroalgal cover from satellite imagery, comparable to results from higher-resolution imagery. However, their predictions were

13

limited to dense stands of homogenous forests, dominated by fucoid species including *Fucus serratus, Fucus vesiculosus* and *Ascophyllum nodosum*. Therefore, the accuracy of their cover estimates is untested in areas that contain more diverse and heterogeneous assemblages. This is important because assemblages with greater diversity and heterogeneity can have more variability in spectral reflectivity, due to the different reflective profiles of individual species, and interactions between species' traits (and reflectance) and the environment (Uhl et al., 2013)

Variation in the spectral characteristic of macroalgae species

Different species of macroalgae show variations in trait expression, including accessory pigmentation that can cause differences in their reflectivity (Rossiter et al., 2020; Schrofner-Brunner et al., 2023; Uhl et al., 2013). Moreover, larger-scale variations in environmental conditions can lead to greater trait variation and spectral reflectivity, making it difficult to accurately predict the total cover of macroalgal forests. Incorporating individual species' reflectivity may enhance the accuracy of total cover predictions, and possibly enable the mapping of macroalgal species. Previous research has outlined the analogous spectral signatures of macroalgal species within the same genus making the separation of species difficult (Uhl et al., 2013). However, a combination of remote sensing and machine learning techniques could distinguish between reflectance profiles of different functional groups (Belgiu & Drăguţ, 2016; DeFries & Chan, 2000; Pham et al., 2023; Rossiter et al., 2020; Uhl et al., 2013). Morpho-functional classification has been widely applied to macroalgal communities due to the difficulty in attaining species-level identification (Balata et al., 2011). Although their effectiveness in assessing spatial-temporal patterns is disputed, previous research has used functional groups to effectively monitor abundance patterns of macroalgae in response to environmental stress (Balata et al., 2011).

Enabling cover predictions of macroalgal groups using machine learning

Rossiter et al. (2020) were able to combine machine learning with UAV imagery to classify areas of macroalgal forests into *Ascophyllum nodosum*, decaying wrack, and mixed *Fucoid* assemblage including *Ascophyllum nodosum* and *Fucus* species (Rossiter et al., 2020). Because of similarities in their morphological traits and spectral characteristics, functionally grouping certain species can improve the predictability of macroalgal spatial extents (Balata et al., 2011; Rossiter et al., 2020; Uhl et al., 2013). Machine learning techniques previously applied to remote sensing include maximum likelihood and random forest classifiers. Maximum-likelihood classifiers determine the likelihood that a pixel belongs to a specific class by using an estimated probability density function, and each class is assumed to have a Gaussian distribution (Foody, Campbell, Trodd, & Wood, 1992). On the other hand, random forest methods are ensemble classifiers. They combine multiple decision tree

classifiers, where each tree is created using a random subset of training data. Individual trees cast unit votes for a class and input vectors are assigned to the class with the most votes (Belgiu & Drăguţ, 2016; Pal, 2005). Random forest classifiers have proven to be effective across a wide range of applications and have the potential to utilise a wide range of spectra information when estimating vegetation spatial extents (Belgiu & Drăguţ, 2016; Pal, 2005). The incorporation of a wider range of spectral information may enable models to predict the cover of specific macroalgal groups with potentially subtle differences in spectral signatures. However, the ability of random forest classifiers to glean information from a wide range of spectral information and the resulting predictive capacity remains poorly tested, especially within intertidal macroalgal habitats. Moreover, although previous attempts have outlined the difficulty in distinguishing between macroalgal species, the ability to identify groups of spectrally distinct macroalgae to gain more functional information from satellite imagery has not been effectively evaluated.
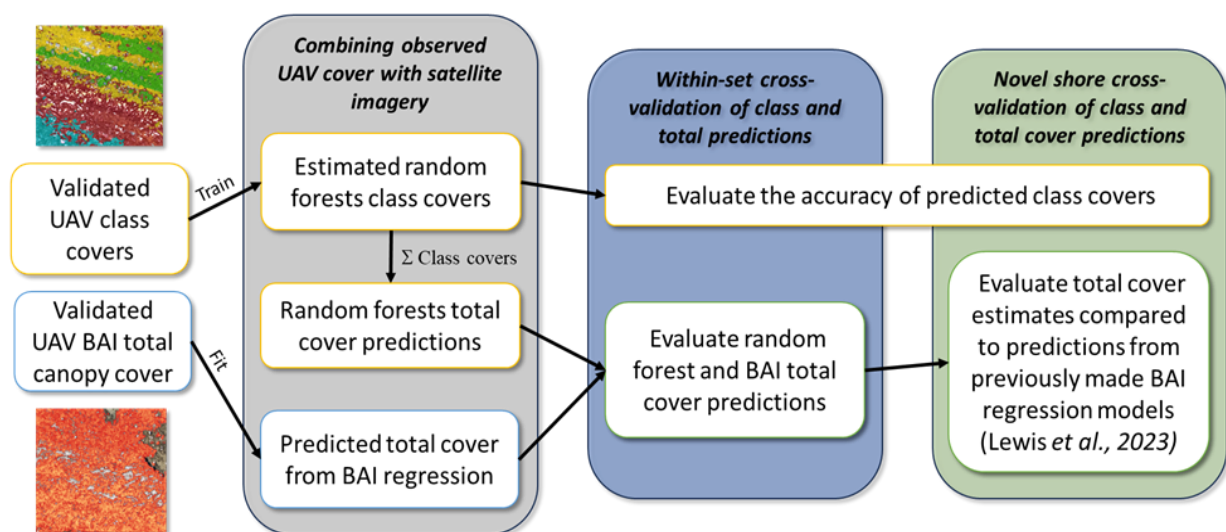
Figure 1: Conceptual methodological workflow. BAI = brown algae Index, UAV = Unmanned Aerial Vehicle. I will first create training data (images, far left) for both the functional group classes and total BAI cover maps based on UAV multispectral imagery, which will be validated using in-situ quadrats. UAV cover estimates will then be related to S2A reflectance values per pixel for random forest models, and S2A BAI values for my BAI regression model (Grey section). Random forests class and total cover estimates will be compared to BAI total cover predictions in two stages, the first using within-set cross-validation (Blue section), and the second using data from two novel shores (Green section). The novel shore estimates from both models created here are finally compared to predictions from previously created BAI regression models (Regression A& B).

Aim and hypotheses

To explore how remote sensing techniques can be most effectively applied to heterogeneous intertidal forests around the UK (Figure 1). To do this 1) machine learning techniques were applied to predict macroalgal functional group cover using Sentinel-2 multispectral imagery. As this is an ambitious and risky undertaking, an alternative approach was tested to estimate the total cover of macroalgae

15

on heterogeneous and diverse shores. Specifically, 2) a BAI regression model based on those outlined by Lewis *et al*. (2023) was re-parameterised across highly heterogenous shores and the predictive power of this model was tested on novel shores.

It was hypothesized that 1) the application of machine learning to incorporate variations in reflectivity between macroalgae species, and the potential use of a greater number of spectral bands, will allow for the classification of key UK macroalgal functional groups from multispectral satellite imagery. Furthermore, it was expected that 2) by combining individual functional group covers the random forest classifier will improve total brown macroalgae cover estimates in comparison with the BAI regression models created using a single vegetation index. Finally, 3) due to the incorporation of greater heterogeneity in model fitting and classifier training, the models created here will more accurately predict total cover compared to previous BAI regression models applied by Lewis *et al*. (2023).
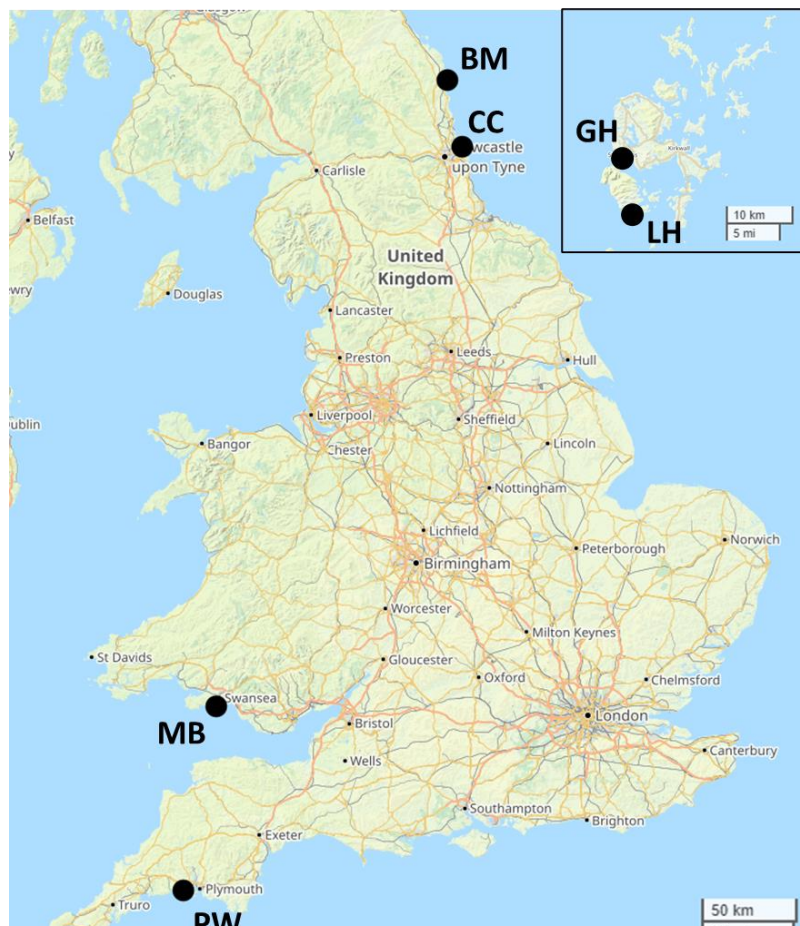
Methods

Figure 2: Sites across the UK and Orkney (top right) where in-situ cover data, UAV and satellite imagery were collected and compared. BM: Boulmer, CC: Cullercoats, GH: Guardhouse, LH: Long Hope, MB: Mumbles, PW: Port Wrinkle. Further site details are outlined in Table 1.
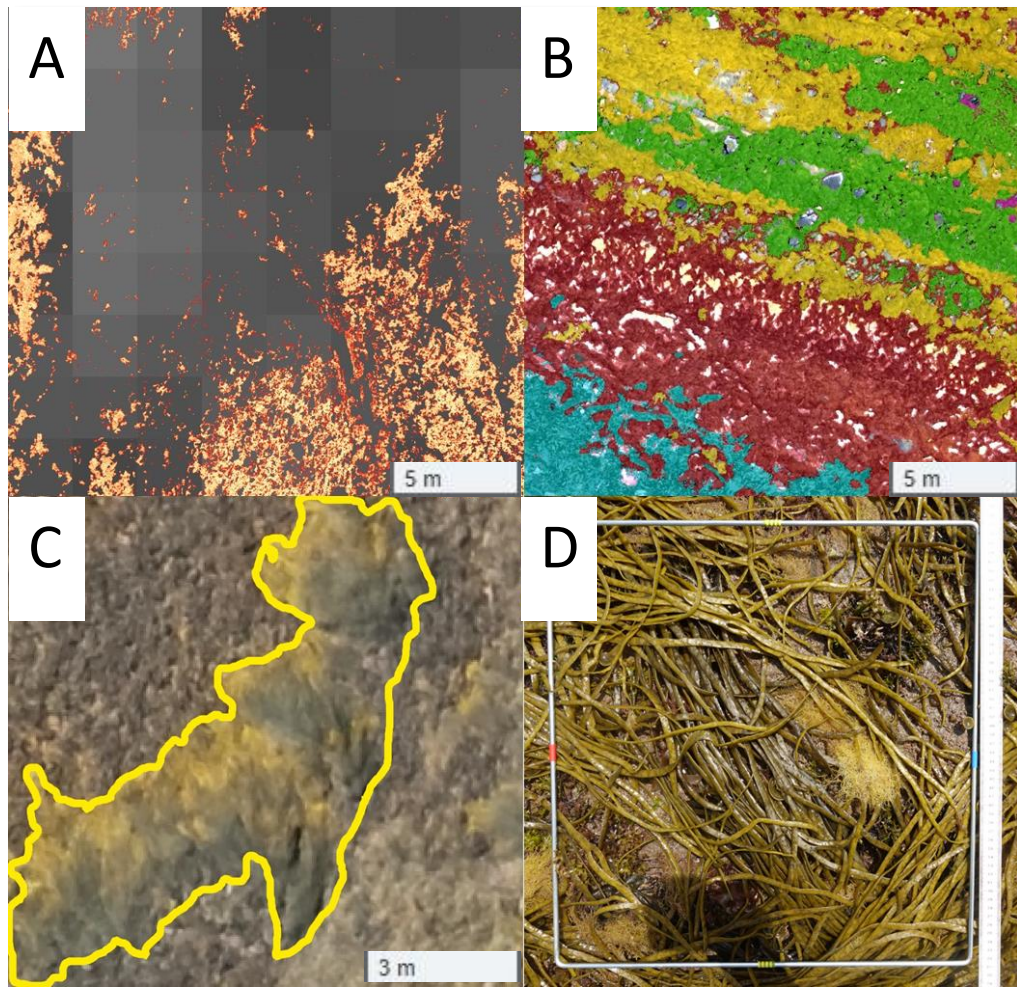
Figure 3: Visual explanation of *in-situ* rocky shore sampling, UAV imagery and classifier techniques. **A**: S2A Near Infra-Red reflectance pixels overlaid with BAI > 4 from UAV imagery. **B**: example UAV macroalgal class map. **C**: Close-up of macroalgal forest showing visual difference in colour and texture between functional groups, outlining *Ascophyllum nodosum* within yellow-highlighted area showing visual differences between older basal parts and newly grown tips, **D**: Method of quadrat (0.5 x 0.5m) picture capture, taken from above and perpendicular to the ground.

In-situ macroalgae cover field survey

Spatial abundances of intertidal macroalgal forests were manually collected for 6 sites, from 4 regions across the UK during the spring/summer of 2022/23 (Figure 2). Sites varied in environmental conditions and macroalgal community. This range of shores included sheltered sites dominated by dense stands of *Fucus serratus* and *Ascophyllum nodosum,* to more exposed shores containing greater diversity of fucoid and kelp species. The location and conditions of each shore are outlined in Table 1, along with dates of image capture. Systematic sampling via grid method was employed at spring water low tide to the top of the intertidal zone at each shore, recording the percentage cover of all species within $0.25m^2$ quadrats. The number of quadrats per shore depended on the horizontal distance between high and low tide. Each shore had between 85 and 100 quadrats, with exception for Mumbles with 114, Portwrinkle with 74, and Long Hope with 53. Images of untouched macroalgae

canopy (larger individuals covering organisms beneath), and sub-canopy (canopy-forming species covered by other species) in quadrats with overlapping species, were taken from above and perpendicular to the ground (Figure 3). Percentage cover was calculated from these images using Vidana image analysis software, created by John Hedley, Marine Spatial Ecology Laboratory, University of Queensland (Version 2, Hedley, 2003). Assemblages encompassed a variety of brown canopy-forming species, including kelps (mainly *Laminaria digitata*), ubiquitous fucoid species (including *Fucus serratus*, *Fucus vesiculosus* and *Ascophyllum nodosum*), to higher shore fucoids such as *Fucus spiralis* and *Pelvetia canaliculata*. Sites were selected for the range of environmental conditions, species diversity, heterogeneity, and coverage of a latitudinal gradient.

Table 1: Dates of multispectral image capture from Sentinel-2 satellite (S2A), and unmanned aerial vehicle (UAV) for each shore. Location and description of each site. Quadrat surveys coincided with the UAV image capture date for each site. CC: Cullercoats, BM: Boulmer, GH: Guardhouse, LH: Long Hope, MB: Mumbles, PW: Portwrinkle.

Shore	S2A image	UAV image	Latitude	Longitude	Region	Conditions	Intertidal macroalgae community	Weather conditios
CC	3/6/2023	3/8/2023	55.03375	-1.428837	North-east England, Newcastle	Moderate to low exposure with estuarine input	Sparse F.spiralis/guiryii and F.vesiculosus patches. Highly abundant canopy of *F.vesiculosus/serratus*, A.nodosum and L.digitata.	Sunny, slight cloud
BM	29/09/2022	12/8/2022	55.42704	-1.577616	North-east England, Newcastle	Moderate exposure with sheltered high shore zones	Extremely large shore. Ranging from sparse to highly abundant cover of F.vesiculosus, A.nodosum and F.serratus.	Overcast, rain
GH	14/06/2023	5/5/2023	58.95092	-3.295285	Orkney, Mainland	High exposure with a large cross-current	Sparse to abundant of F.spiralis/guiryii cover. Abundant cover of F.vesiculosus and A.nodosum. Highly abundant cover of F.serratus, L.digitata, S.latissima and A.esculenta.	Sunny, clear
LH	14/06/2023	18/05/2023	58.7798	-3.22849	Orkney, Hoy	Low exposure within sheltered bay	Spare patches of P.canaliculata. Sparse to abundant F.spiralis/guiryii patches. Abundant to highly abundant cover of F.vesiculosus, A.nodosum and F.serratus.	Overcast, heavy rain
MB	12/8/2022	15/07/2022	51.5663	3.980094	South-West Wales, Swansea	Moderate to high exposure with estuarine input	Sparse to abundant patches of F.spiralis/guiryii and P.canaliculata. Sparse to abundant patches of F.vesiculosus/serratus and A.nodosum.	Sunny, clear
PW	29/09/2022	4/7/2023	50.36104	-4.310688	South-West England, Cornwall	Moderate to high exposure	Spare patches of F.spiralis/guiryii and A.nodosum. Sparse to abundant patches of F.vesiculosus and F.serratus. Sparse patches of L.digitata.	Sunny, clear

UAV image collection and processing

UAV imagery was captured with a 5-band multispectral optical camera (capturing RGB image along with Red [R], Green [G], Blue [B], Red edge [RE] and Near-Infrared [NIR] as individual bands) mounted on a DJI Phantom 4 Pro UAV (DJI, Shenzhen, China). Flights were at an altitude of ~50m, with 80% side overlap, 70% forward overlap, and an image capture interval of 2s, giving a speed of ~17km/h, producing a ground sampling distance pixel size of ~2.5cm. DJI GS Pro was used to create the flight plans, completed at the lowest possible tide mark during mean low water spring tides during the spring and summer months of 2022/23. All flight dates and times are shown in Table 1. Digital surface models and reflectance-corrected orthomosaics were created using Pix4Dmapper Ground Control Points were used for differential-GPS correction, with around 6-9 locations at each site recorded using an EMLID reach RS2 GNSS GPS. The final products were sets of reflectance maps,

18

including RGB combined sensor, each spectral band; B [450nm], G [560nm], R [650nm], RE [730nm], NIR [840nm], and a digital surface model. Each pixel within the reflectance maps represents a calibrated value of the object's reflectance or physical information such as shore height. All outputs used the coordinate reference system WGS84/UTM zone 30N. The intertidal region of each shore was partitioned using normalized difference water index and visual assessments, feasible due to the high resolution of UAV images and elevation from the digital surface model. This removed the interference on reflectivity from large areas of standing water, particularly in the NIR wavelength critical in classification (Bell et al., 2020; Malthus & George, 1997).

Satellite image collection

Sentinal-2 level-2A (S2A) imagery was obtained from Copernicus, European Space Agency (ESA). Cloud-free images, corresponding with mean spring low water and *in-situ* sampling between May-Sep, were selected for each site's sampling year (Table 1). The time between UAV and satellite image capture for each shore was dependent on the availability of cloud-free images captured during a low tide. Downloaded S2A images comprise of 12 individual bands (Coastal Aerosol [CA], Blue, Green, Red, RE1, RE2, RE3, NIR, narrow-NIR [nNIR], Water Vapour [WV], Shortwave Infra-red 1 [SWIR1], SWIR2), with resolution ranging from ~36-100m^2. ESA imagery is corrected using Sen2Cor processor (v2.5.5, European Space Agency).

UAV classification maps

The maximum likelihood classifier from the Semi-Automatic Classifier Plugin within QGIS (version 3.34.0) estimated the spatial extents of specified classes. The final classes were selected based on the spectral separateness of the macroalgal species found across all the sites. Spectral separateness was assessed using the Semi-Automatic Classifier. Species of the same genus, which could not be separately identified using multispectral imagery, were merged into functional groups (Congedo, 2021; Rossiter et al., 2020; Uhl et al., 2013). Maximum-likelihood classification is a popular classifier based on a probability density function, assuming a Gaussian distribution of each spectral class (Foody et al., 1992; Paola & Schowengerdt, 1995; Shivakumar & Rajashekararadhya, 2018).

Image-derived training data was obtained from the aligned multispectral imagery, using visual identification of target features (set macroalgae functional group classes) and the manipulation of training polygons over areas of known class cover (Middlekoop and Addink, 2018; Rossiter 2020). The number of polygons per class depended on the number of clear homogenous areas identified, with a minimum of 100 pixels per class for adequate classification, and classes were chosen due to spectral separateness (Middlekoop and Addink, 2018). Edge effects were noted at boundaries between classes, often incorrectly identified or unidentified, similar to results found in Rossiter et al. (2020)

and were manually re-coded. *Ascophyllum nodosum* was visually and spectrally distinct, and so created an individual class of their own. *Pelvetia canaliculata* and *Himanthalia elongata* also comprised individual classes, although both had a low number of recorded samples. Kelp species including *Laminaria digitata, Saccharina latissima* and *Alaria esculenta* were grouped, and *Fucus* species were split into two classes: *F. vesiculosus/F. serratus* and *F. spiralis/F. guiryii* because each group was spectrally distinct, whereas species within them could not be confidently separated. The combination of maximum likelihood classifier and manual identification was highly supervised to create the most accurate 'known' class covers possible for training the random forest model predictions from satellite imagery.

To validate the mapped class covers, the 'known' species cover recorded from *in-situ* quadrats were compared to the estimated classifier cover (Figure 4). The same was performed for the total cover estimates using the brown algae index (BAI). A BAI threshold of between 4 and 5 was used depending on the shore, as the previous set threshold of 4 required adapting to best reflect the observed cover present at each site (Lewis et al., 2023). Equation 1 shows the method of calculating the BAI.

$$\text{Brown algae index} = \text{NIR/G} \qquad (1)$$

Satellite cover estimates

Four sites were selected to train the random forest models, because they covered a range of species diversity and community heterogeneity. The training sites were Cullercoats (CC), Guardhouse (GH), Long Hope (LH) and Mumbles (MB) (Figure 2). These shores ranged from habitats containing larger monoculture stands of canopy forming macroalgae, such as Long Hope, to more exposed sites like Mumbles, which contain mixed stands of multiple species more intermittently spread across the shore. Furthermore, the four sites are spread geographically across the UK and range in levels of exposure (Table 1, Figure 2). Sentinel-2 (S2A) images were resampled to 100m^2 resolution, to match the minimum resolution of S2A imagery, then aligned to UAV mosaics. To remove interference on reflectance values by standing water, images were clipped to the rocky intertidal area above the low tide mark. Class percentage cover was calculated as the proportion of pixels assigned to each class to the total number of pixels within each 100m^2 area (corresponding to individual pixels from the Sentinel-2 satellite images). This calculation is expressed in Equation 2, where x = the number of pixels of a present class and, y = the number of total pixels.

$$\text{Percentage cover of each class per quadrat or S2A pixel } = (x / y) \text{ x } 100 \qquad (2)$$

Random forest classifiers were used to predict individual class covers per 100m^2 pixel using S2A reflectance values from the 12 available bands, and the total brown canopy cover was the sum of all the predicted class covers. Predicted total brown macroalgal cover from the random forest classifier was compared to estimates from the BAI regression models. The same four shores were also used to fit a new polynomial BAI regression model following methods outlined by Lewis et al. (2023). A quadratic polynomial regression was applied to the BAI reflectance value per 10 x 10m satellite pixel as a function of validated observed total brown macroalgal cover, from UAV imagery. The coefficients were then extracted and used to create the quadratic polynomial equation to predict cover from using BAI reflectance values (Table 2).

Table 2: Quadratic polynomial regression formulae of each BAI model to predict % cover within each 10 x 10m Sentinel pixel. X = BAI reflectance value of the pixel. The values shown were extracted from polynomial regression of the validated observed total brown macroalgal cover, from UAV imagery, as a function of BAI reflectance value per 10 x 10m satellite pixel.

Equation	Formula
Regression A	% Cover = $-2.7542x^2 + 15.679x + 71.234$
Regression B	% Cover = $-0.8619 x^2 + 9.6001x + 69.145$
New BEF Regression	% Cover = $-0.7824 x^2 + 9.1155x + 77.104$

Because the multiplicative factors within the polynomial model are created from the relationship between component variables (BAI reflectance and percentage cover), there is inherent covariance within the models, potentially exaggerated by multiplicative terms. BAI reflectance values from S2A images were therefore centred (subtracting each value by the mean) to lessen the correlation between the multiplicative terms and the component variables being multiplied within the quadratic polynomial model. This also eases model interpretation, by avoiding the creation of very large outliers created from the multiplication terms. Independent variables (S2A BAI values) lower than those used to create each regression model (<-5.4 for my BAI regression, <-3.03 for Regression A and <-4.41 for Regression B) were assigned 0% total brown algal cover while those higher BAI values (>6 my BAI regression, >3.76 for Regression A and >6.01 for Regression B) were assigned 100% total brown algal cover.

Satellite cover validation

To validate both the random forest classifiers and regression models, two sets of known spatial abundance data were utilised. First, the data from the four shores was split in half and used the first 50% for model training. Within-set cross-validation was the applied using the remaining 50% of the data. This tested the ability of random forest models to accurately predict functional group cover from

S2A images and compare total canopy cover estimates from both models at a range of naturally occurring diversity and heterogeneity. For the second validation step, both methods trained on the entire dataset from the four training shores were applied to 8600m^2 from two novel shores unused in model training. This stage assessed model predictions on novel shores with different environmental conditions. This is a crucial test of model estimates as researchers and managers are likely to want to use satellite data to estimate intertidal forest (and component functional groups) cover at sites that lack extensive ground/training data. Similarly to training images, any large areas of standing water were removed due to interference in reflectance values. In addition, ~140m^2 of rocky shore was removed due to the presence of decaying wrack. Both validation stages have been utilised in previous remote sensing research on macroalga forests (Kotta et al., 2018b; Lewis et al., 2023). Lastly, total cover predictions from both my BAI regression and random forest models were tested against two previously used BAI regression models applied by Lewis *et al*. (2023) (Regression A & B hereafter). Regression A and B were fitted and validated using 3 shores in Mid Wales containing similar homogenous macroalgal assemblages of *Fucus vesiculosus*, *Fucus serratus* and *Ascophyllum nodosum* (Lewis et al., 2023) Site one was situated near Aberystwyth, with a visually estimated coverage of >80% canopy, comprised of *Fucus vesiculosus*, *Fucus serratus* and *Ascophyllum nodosum* (Lewis et al., 2023) Whereas, sites two and three were around 10km north of Aberystwyth, containing a spare to abundant (0-80%) cover of *Fucus vesiculosus* and *Fucus serratus* (Lewis et al., 2023). Comparison of the models created by Lewis *et al*. (2023) to the BAI models created here enabled the evaluation of any increases in predictive power by the inclusion of a greater range of natural heterogeneity and diversity within training data.

Statistical analysis

The observed percentage cover of random forest functional classes and BAI total canopy cover from UAV imagery was combined with S2A imagery and extracted using QGIS (version 3.34.0). BAI regression and random forest models were created, and cover estimates analysed, using R (version 4.3.1; R Core Team, 2023). The predicted cover from S2A imagery was compared to UAV observed covers. This was done using R^2 values and root mean square error of the difference between the estimated satellite cover and observed cover from UAV imagery. Linear model assumptions of the BAI regressions were evaluated using residual and histogram plots.

Results

Accuracy of UAV cover maps using maximum likelihood classifier or BAI

UAV-mapped covers using both maximum likelihood classifiers and BAI showed high accuracy when validated against observed cover measured from *in-situ* quadrats at all six sites (Table 1, Figure 4).

All cover predictions showed R^2 values of > 0.95 and RMSE of < 5.7, for random forests class covers and total cover estimated by both the BAI regression and random forest classifier (Figure 4). Visual validation, and low RMSE values, established the UAV classification maps as an accurate representation of the functional classes and BAI total spatial extents. These spatial extents were therefore used as 'known' cover values to compare against satellite estimates.
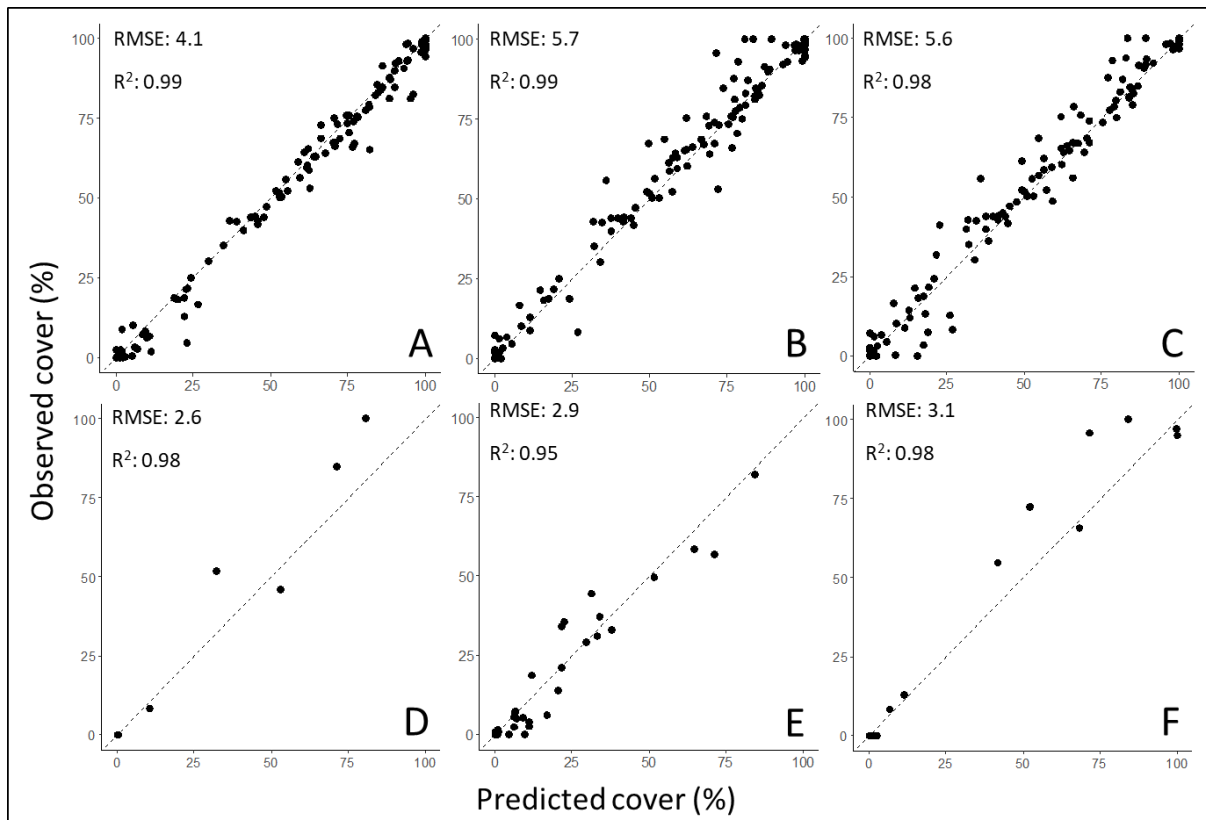

Figure 3: Predicted vs observed cover within in-situ 0.25m^2 quadrats. Predictions of **A**: BAI regression total cover, **B**: random forests classifier total cover. Random forests class cover for **C**: Fucus serratus/vesiculosus, **D**: Kelp, **E**: Ascophyllum nodosum, & **F**: Fucus spiralis/guiryii. RMSE and R^2 values corresponding to each plot represent the overall accuracy of the model's predictions. Details of all six sites can be found in Table 1.

Functional group classification

During the first validation step, random forest models were able to accurately predict cover for all classes (Figure 5), particularly for those with high levels of collected cover data, including *Fucus serratus/vesiculosus* (RMSE: 10.3, R^2: 0.89), *Ascophyllum nodosum* (RMSE: 7.1, R^2: 0.72), Kelps (RMSE: 4.7, R^2: 0.90), and *Fucus spiralis/guiryii* (RMSE: 5.7, R^2: 0.71). Weaker cover estimates were produced for the less abundant classes of *Himanthalia elongata* (RMSE: 1.6, R^2: 0.63) and *Pelvetia canaliculata* (RMSE: 0.1, R^2: 0.43). With exception of Long Hope (LH), the Random Forest classifier was able to accurately predict the cover of the four most abundant functional groups: Fucus, Asco, Kelp and Spirguy (Table 2). As shown in Table 2, RMSE values for these four main functional

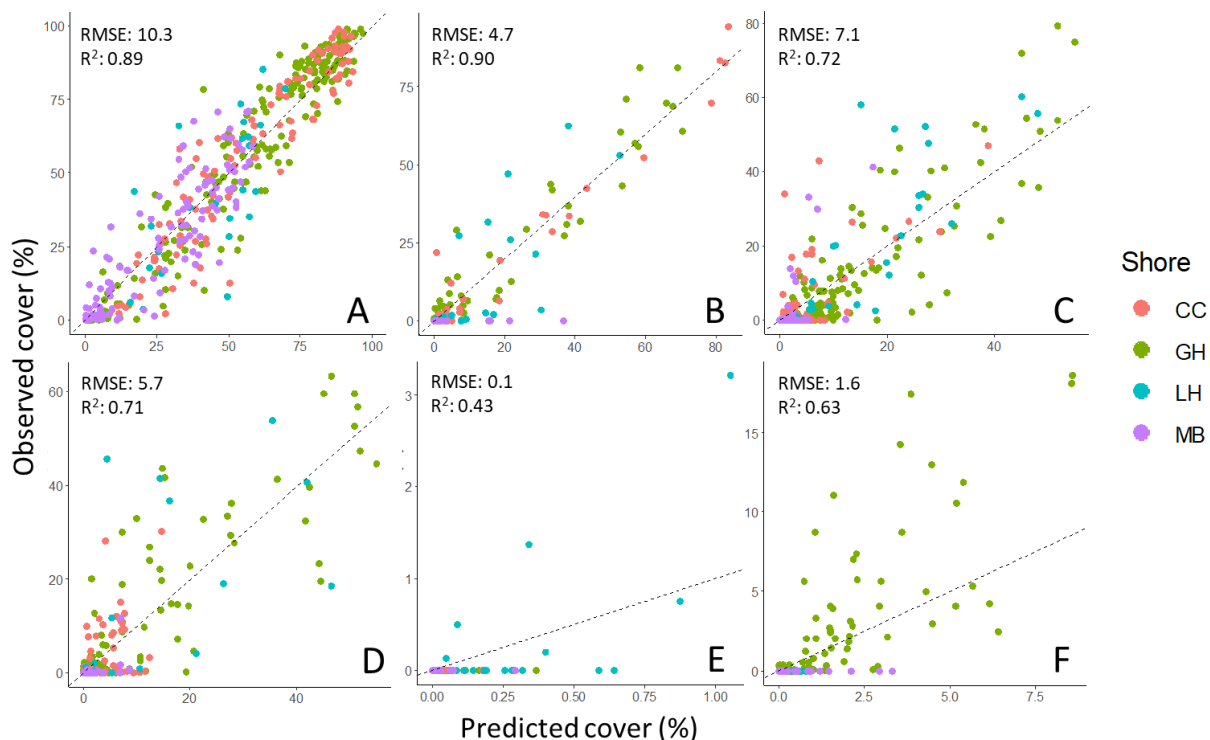group predictions were consistently lower than 10 at three of the four shores used in validation stage one.

Figure 4: Predicted vs observed percentage cover per 100m2 pixel area, estimated using a combination of 12 possible S2A reflectance band values for 50% of the four training shores (Validation stage 1). Random forests estimated class covers for **A**: *Fucus vesiculosus/serratus*, **B**: Kelp, **C**: *Ascophyllum nodosum*, **D**: *Fucus spiralis/guiryii*, **E**: *Pelvetia canaliculata*, **F**: *Himanthalia elongata*. RMSE and R2 values corresponding to each plot represent the overall accuracy of the model's predictions. Each pixel estimate is colour-coded to individual shores (CC: Cullercoats, GH: Guard House, LH: Long Hope, MB: Mumbles). Details of all six sites can be found in Table 1.

Table 2: Performance indicators of Random Forest species predictions for individual shores used in validation stage one and two. Critically, with exception of Long Hope and Boulmer, the four functional groups with enough cover to confidently analyse predictions (Fucus, Asco, Spirguy and Kelp) showed RMSE values consistently lower than 10. N/A values represent no cover of a species at the shore.

	Fucus		Asco		Spirguy		Pcan		Helo		Kelp		TotalB	
Shore	RMSE	R2	RMSE	R2	RMSE	R2	RMSE	R2	RMSE	R2	RMSE	R2	RMSE	R2
CC	10.013	0.888	6.218	0.499	4.479	0.238	0.024	N/A	0.074	N/A	3.317	0.965	9.373	0.865
GH	9.393	0.919	7.207	0.790	6.004	0.800	0.043	N/A	2.268	0.626	3.950	0.938	8.801	0.901
LH	17.280	0.459	14.166	0.594	13.242	0.440	0.540	0.455	0.241	N/A	11.174	0.648	12.308	0.071
MB	10.404	0.762	4.907	0.429	1.553	0.304	0.031	N/A	0.584	N/A	4.359	N/A	13.516	0.599
BM	23.917	0.170	13.024	0.129	1.368	N/A	0.004	N/A	0.328	N/A	0.764	N/A	15.901	0.236
PW	9.108	0.727	7.907	0.339	2.654	0.191	0.006	N/A	1.812	N/A	3.597	0.714	12.088	0.657

During the second validation stage however, only *Fucus serratus/vesiculosus*, (RMSE: 15.6, R^2: 0.90) and Kelp (RMSE: 3, R^2: 0.71) cover could be accurately predicted on novel shores, with weaker estimates of *Fucus spiralis/guiryii* (RMSE: 2.3, R^2: 0.43) (Figure 6). For the remaining classes, accurate cover predictions were not produced. However, models were able to identify the relative absence of *Pelvetia canaliculata* and *Himanthalia elongata* compared to the previously mentioned more abundant classes (Figure 6). *Himanthalia elongata* cover predictions were constrained to <7% (with the majority <2.5, RMSE: 1.5), and all *Pelvetia canaliculata* predictions were <0.05%, RMSE: 0.005). *Ascophyllum nodosum* was the only species that the random forest models failed to predict percentage cover on novel shores (Figure 6). When separated by shore, species cover predictions showed greater performance at Portwrinkle compared to Boulmer for the four most abundant functional classes: Fucus, Asco, Kelp and Spirguy (Table 2). Critically, RMSE values for Fucus, Kelp and Spirguy at Portwrinkle were lower than 10, outlining similar levels of accuracy shown in validation stage one.
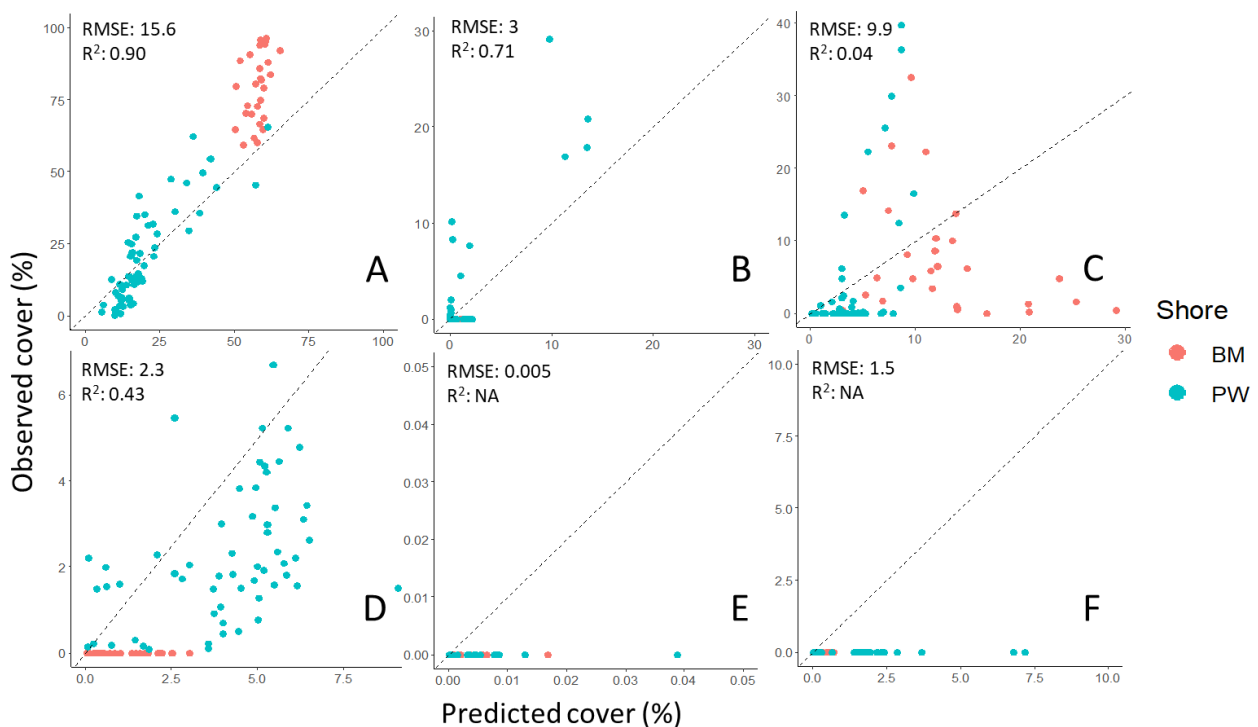
Figure 5: Predicted vs observed percentage cover per 100m2 pixel area, estimated using a combination of 12 possible S2A reflectance band values from two novel shores (Validation stage 2). Random forests estimated class covers for A: *Fucus.vesiculosus/serratus*, B: Kelp, C: *Ascophyllum nodosum*, D: *F.spiralis/guiryii*, E: *Pelvetia canaliculata*, F: *Himanthalia elongata*. RMSE and R2 values corresponding to each plot represent the overall accuracy of the model's predictions. Each pixel estimate is colour-coded to individual shores (BM: Boulmer, PW: Port Wrinkle). Details of all six sites can be found in Table 1.

Functional group classification error

Ascophyllum nodosum predictions were the main source of inaccuracies from the random forest classifier (Figure 6, C). This was thought to be due to intra-species variation in reflective signatures within *Ascophyllum nodosum* individuals (from lower to upper portions of their long fronds; Figure 3). Thus, reflectance profiles were assessed from a subset of 129 *Ascophyllum nodosum* samples from all the shores and related to individual lengths. Figure 7 shows the difference in reflectance of *Ascophyllum nodosum* individuals at the 2 novel validation shores compared to the 4 training shores. A lower mean reflectance of red edge can be seen at PW, along with a greater mean reflectance and variation in the near-infrared at BM (Figure 7). Moreover, the increased spectral variability expressed by *Ascophyllum nodosum* corresponds to older and larger individuals (Table 3).
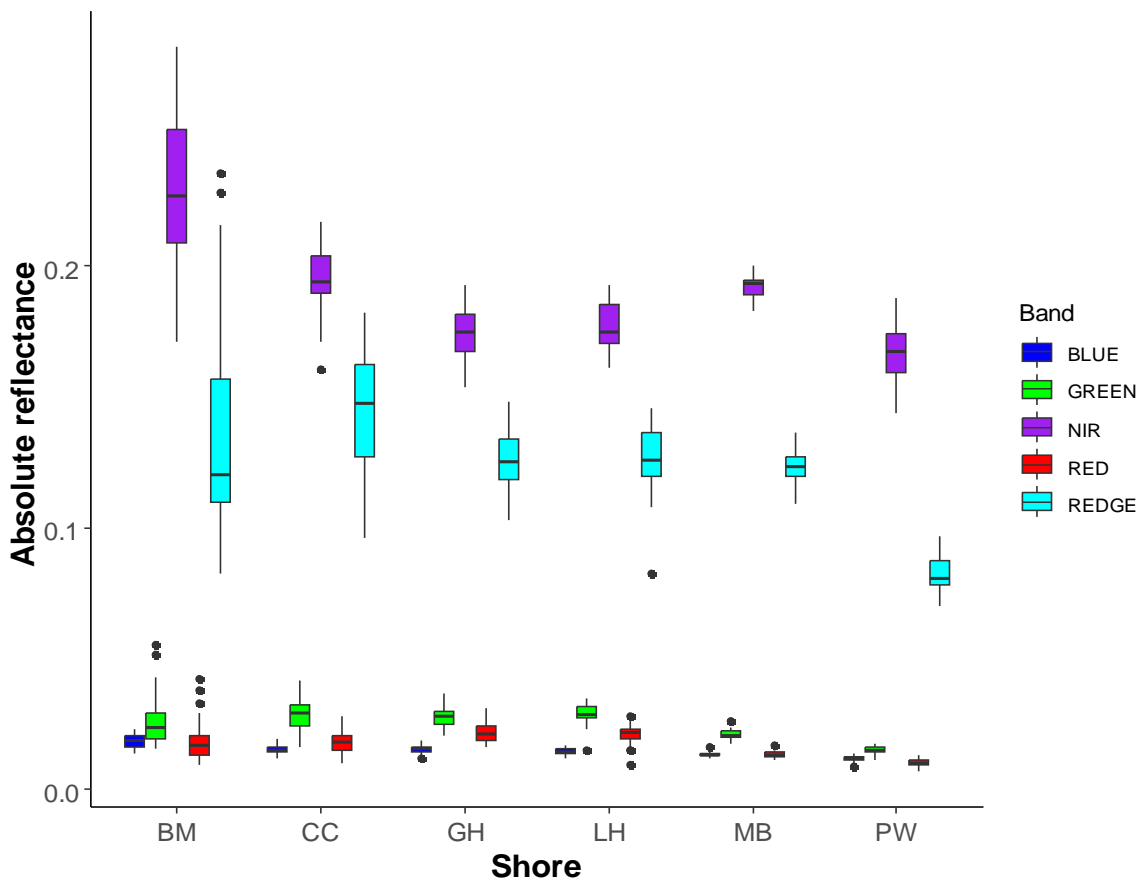
Figure 6: Variation in reflectance of *Ascophyllum nodosum* individuals across the 4 training shores: Cullercoats (CC), Guardhouse (GH), Long Hope (LH) and Mumbles (MB), and 2 novel validation shores: Boulmer (BM) and Port Wrinkle (PW). Highlighting the greater variation within the absolute reflectance of Red-edge (REDGE) and Near Infrared (NIR) bands at BM, and lower average Red-edge at PW. Details of all six sites can be found in Table 1.

Table 4: The relationship between individual length of *Ascophyllum nodosum* (mm), and variation in spectral reflectance values of the Near-Infrared (NIR) and Red-Edge (RE) band represented by standard deviation (SD) at each site.

Shore	Average length (mm)	Length SD (mm)	RE absolute reflectance SD	NIR absolute reflectance SD
BM	973.875	380.527	0.042	0.032
CC	837.111	222.113	0.021	0.014
GH	701.120	271.372	0.011	0.011
LH	713.818	202.947	0.014	0.009
MB	703.375	183.748	0.007	0.004
PW	445.000	65.058	0.008	0.011
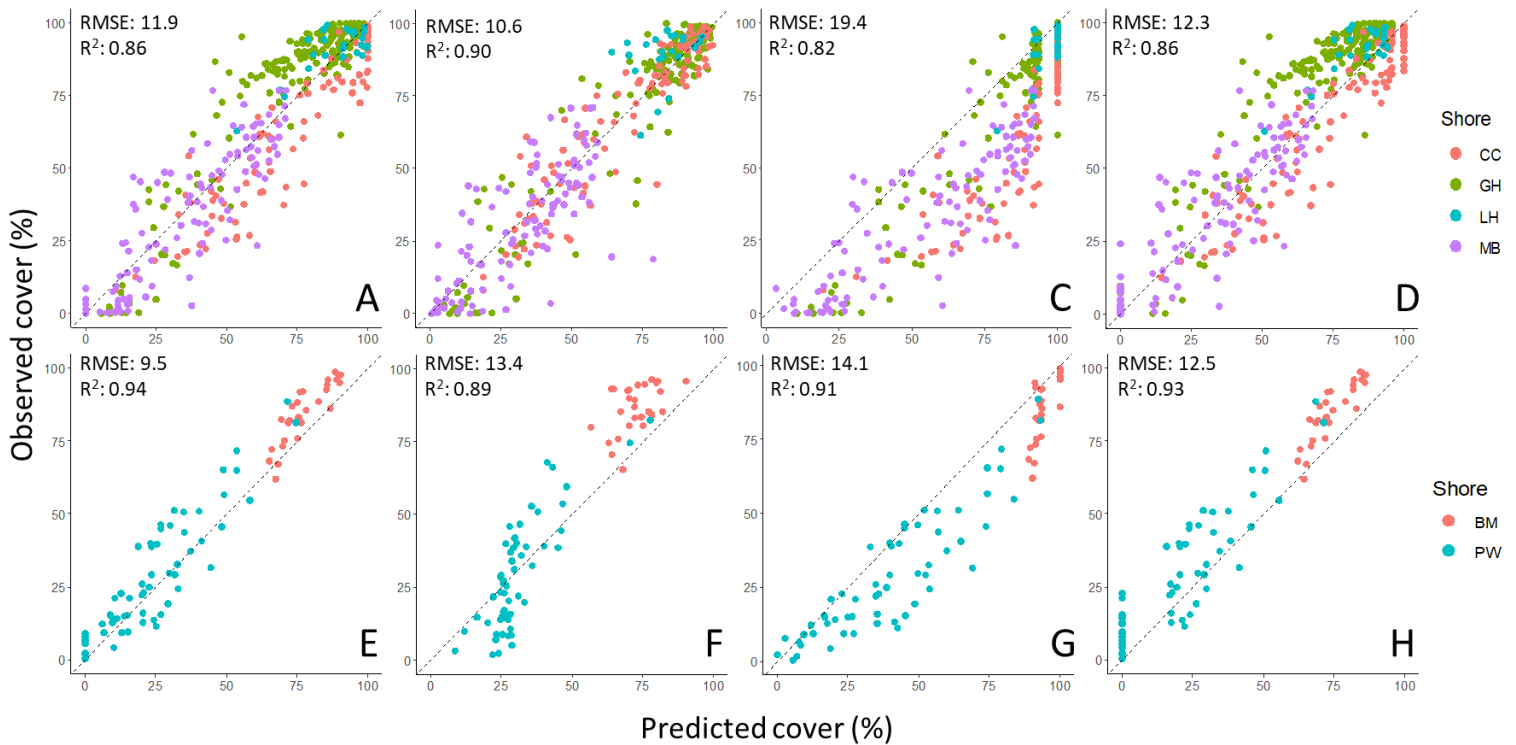
Figure 7: Predicted vs observed total canopy cover per 100m2 pixel area, estimated using a combination of 12 possible S2A reflectance band values. First for 50% of the four training shores (Validation stage 1) from A: BAI regression model made here, B: Random Forest classifier, C: Lewis et al. (2023) regression A, D: Lewis et al. (2023) regression B. The same applied to the novel shore data (Validation stage 2) from E: BAI regression model made here, F: Random Forest classifier, G: Lewis et al. (2023) regression A, H: Lewis et al. (2023) regression B. With RMSE and R2 values representing the overall accuracy of each model's predictions. Each pixel estimate is colour-coded to individual shores (CC: Cullercoats, GH: Guard House, LH: Long Hope, MB: Mumbles) and (BM: Boulmer, PW: Port Wrinkle). Details of all six sites can be found in Table 1.

Total canopy cover estimates

The first validation stage, using the remaining half of the data from the training shores, found both random forest and regression models had similar accuracy in the estimation of total brown canopy-forming macroalgae, with a slight improvement in the random forest predictions (RMSE: 10.6, R^2: 0.90) compared to the BAI regression model (RMSE: 11.9, R^2: 0.86) (Figure 8). From these results, it can be concluded that mapping individual reflectance profiles of functional groups slightly improved brown canopy estimates compared to BAI regression. However, this is limited to 'similar' shores (shores with comparable characteristics including community compositions and environmental conditions etc) as when both models were applied to novel shores BAI regression predictions performed better than those from the random forest (RF) classifier, with improved R^2 and RMSE

values (BAI: RMSE: 9.3, R^2: 0.94; RF: RMSE: 12, R^2: 0.89).

Both BAI regression and random forest models created here estimated total cover more accurately than previously used BAI regression models applied by Lewis *et al*. (2023). Figure 8 shows Regression A from Lewis *et al*. (2023) greatly overpredicted total cover (RMSE: 63.8, R^2: 0.94), whereas Regression B from Lewis *et al*. (2023) performed comparatively better (RMSE: 17.1, R^2: 0.92) though still consistently underpredicting total cover. Moreover, the better-performing Regression B showed aggregations of predictions around 0% with corresponding observed cover values up to 25%. Similar aggregation is shown around 100% for Regression A, although less pronounced. This clustering is because BAI regression models are unable to predict pixels with BAI values outside fitted model limits, which are automatically bounded at 0% but contain higher observed percentage covers. Overall, the BAI regression model re-parameterised here was the best technique for estimating total brown macroalgae cover on novel shores.

Discussion

Functional group cover estimates

Here, machine learning models could identify the community composition of intertidal macroalgal forests at the functional group level from satellite imagery, by using random forest classifiers to select important cover predictors from a wide range of spectral information. Similar methods have previously been employed to map macroalgae to lower taxonomic distinctions, such as to the Family or Genus level (Brodie et al., 2018; Rossiter et al., 2020). However, this was achieved with higher resolution aerial or UAV imagery, whereas the separation of multiple functional groups (or "unmixing") has not been previously attained from multispectral satellite imagery. This contrasts

previous work using multispectral satellite imagery to map intertidal macroalgae, in which cover predictions have been limited to the identification of a single broad vegetation class per pixel (Lewis et al., 2023; M. Wang & Hu, 2021). These efforts have been predominantly limited to separating macroalgal phyla (green, brown, and red algae) due to evidence highlighting the pronounced spectral differences between them (Kotta et al., 2018; Lewis et al., 2023; Uhl et al., 2013). Although random forest models could not consistently provide accurate cover estimates on novel shores for all classes, they could provide information on the community composition of functional groups within each shore from satellite multispectral images, except for *Ascophyllum nodosum*.

Functional group validation

During the first validation stage, random forest classifiers simultaneously predicted the cover of multiple functional groups on within-set shore data, with root mean squared errors (RMSE) of 10 or below (Figure 5), outlining the ability of random forest models to predict the cover of multiple functional groups from satellite imagery on shores with similar environmental conditions and macroalgal species to those used during model training. However, the second validation stage is the more credible evaluation of model predictability for widespread application to satellite imagery, as it used images from novel shores independent from the training data. Here the random forests classifiers only produced accurate cover predictions for *Fucus serratus/vesiculosus* (RMSE 15.6, R^2 0.95) and Kelp (RMSE 3, R^2 0.84) as shown in Figure 6. Weaker predictions were observed for *Fucus spiralis/guiryii* (RMSE 2.3, R^2 0.43), predominantly due to this class's observed patchiness of cover (Figure 6). Both *Himanthalia elongata* and *Pelvetia canaliculata* were absent at the novel shores used for the second validation stage, thus the ability of random forests models to accurately predict the cover of these classes cannot be fully validated. However, cover predictions for both were consistently below 7.4% and 0.04% for *Himanthalia elongata* and *Pelvetia canaliculata* respectively, therefore random forest models consistently predicted low abundances for these absent classes (Figure 6). These results highlight the necessity for improvements to random forest classifiers required to increase the robustness of their predictions of functional group cover when expanding efforts to novel shorelines that may contain variations in reflectivity not captured within training data. This increased error at the functional group level translated further into a lower accuracy of total cover estimates during the second validation stage from the random forest classifier compared to BAI regression outputs.

Total cover estimates from random forest classifiers

Overall, the random forest classifier showed lower robustness when estimating total brown macroalgal cover compared to the BAI regression model created here. Random forest predictions

showed greater accuracy during within-set validation (RMSE: 10.6) compared to the BAI regression created using the same training data (RMSE: 11.9) (Figure 8). This may be due to the iterative nature of random forest models which allows for the potential inclusion of a greater range of spectral information during model training compared with index-linked approaches (Belgiu & Drăguţ, 2016; Pal, 2005). For instance, Blue and Red Edge bands can correspond to peaks in the reflectance profiles of certain macroalgal species (Uhl et al., 2013). The model can then account for the relationship between reflectivity and level of cover differently for each algal class. However, the random forest classifier showed reduced consistency during predictions on novel shore data (RMSE: 13.4) in comparison with BAI regression predictions (RMSE: 9.5; Figure 8). The reduced accuracy of the random forests model identifies the possible errors in predictions using machine learning algorithms to tailor cover estimates to specific functional groups using a greater number of spectral bands while outlining the robustness of BAI regression estimates.

Random forest classifier error and improvement

The reduced accuracy of random forest predictions on the novel shore data could be evidence of the model's overfitting to the training data, which can be reduced by increasing the amount and quality of training data (DeFries & Chan, 2000; Pal, 2005). Improving the quality of known cover data could be accomplished by employing other classifiers at the UAV level that are better suited to the multi-modality of multispectral data compared to maximum likelihood techniques. In addition to random forest classifiers, methods such as Support Vector Machines and Artificial Neural Networks do not make assumptions on data distribution, which increases their applicability to remote sensing data (Belgiu & Drăguţ, 2016). Alternative methods such as these could remove errors apparent in the distributions of the created UAV class maps (Figure 4), which may have introduced further errors in the random forest predictions from satellite imagery. Evidence of this could be found in the RMSE values separated by shore, as Long Hope and Boulmer showed consistently higher error in all predicted classes (Table 2). Both Boulmer and Long Hope had overcast and rainy conditions during the drone image capture, in comparison to clear sunny days at the remaining sites. The poor conditions may have introduced differences in reflectivity of all macroalgae present, leading to errors in the 'known cover' maps. Further application of the Random Forest model to more sites with clearer conditions during drone flight may allow for greater validation the models spatial transferability. Alternatively, Belgiu & Drăguţ (2016) outlined the reduced variance and bias of random forest classifiers using boosting methods such as AdaBoost or JointBoost, compared to the bagging methods utilised here. These general techniques can be employed to improve the classifier predictability on novel data and reduce potential model overfitting. However, a main attribute of ensemble classifiers is the ability to reduce the likelihood of overfitting (Belgiu & Drăguţ, 2016; DeFries & Chan, 2000;

Pal, 2005). Therefore, the main source of reduced accuracy on novel imagery most likely came from the variation of reflectivity within species due to trait differences between individuals in varying environmental conditions.

Reflectivity and intra-species trait variation

During validation on independent novel shore data, *Ascophyllum nodosum* was the only class in which predictions showed no relation to those observed from UAV imagery. This is predominantly due to intra-species variation of spectral responses between individuals of *Ascophyllum nodosum* not accounted for by the random forest model. *Ascophyllum nodosum* is a long-lived and slow-growing fucoid species, and Figure 3 shows the visible difference between darker basal frond areas compared to the lighter-growing tips of large individuals. This translates to a greater variation in reflectivity in larger *Ascophyllum nodosum* individuals (Table 3), especially in Near Infra-Red (NIR) and Red Edge (RE) wavelengths (Figure 7). Previous work has identified both the visual difference in colouration and spectral variation within and between individuals of the same species of brown macroalgae (Uhl et al., 2013). Furthermore, Timmer *et al.* (2024) found similar variations of reflectivity within RE and NIR bands of kelps containing large buoyancy structures (airbladders) within their fronds, which are also present in *Ascophyllum nodosum* (Timmer et al., 2024). Although more pronounced in *Ascophyllum nodosum,* seasonal differences and expansion to new regions may reduce the predictive power of random forest models due to trait differences altering reflectance characteristics of all brown canopy-forming macroalgae (Schrofner-Brunner et al., 2023; Uhl et al., 2013). In addition to differences in reflectivity, the greater size of macroalgae individuals can decrease the accuracy of predictions due to differences in where the algae lay after tidal inundation. An impact that would be exacerbated by the time elapsed between the dates of capture of the UAV and satellite images, due to the variation in weather conditions or tidal cycle. This may also explain the reduced accuracy at Boulmer (Figure 6), as this shore had the largest individuals of *Ascophyllum nodosum* in areas mixed with other Fucoid species (Table 3). Furthermore, both Boulmer and Long Hope were the only two shores dominated by *Ascophyllum nodosum, Fucus vesiculosus and Fucus serratus* from the upper middle shore to the low tide mark. This community structure is due to the different environmental conditions at these sites, compared to the other four used here, specifically the low exposure. In turn, the traits of the individuals at Boulmer and Long Hope may have significant differences in reflectivity not properly integrated into the model, leading to increased error at these sites (Table 2). Future work should attempt to incorporate intra-species trait variation, such as the impact of frond length on accessory pigment concentration, to improve model predictions in novel regions and temporal datasets.

Total cover estimates from BAI regression models - incorporating greater diversity and heterogeneity

BAI regression models provided robust total brown macroalgal cover estimates, showing greater accuracy on novel shores compared to the random forest classifiers (Figure 8), outlining the proficiency of the index-based approaches in estimating brown algal cover from satellite imagery created by Lewis *et al.* (2023). Furthermore, my BAI regression model created here showed improved accuracy of total cover predictions in both validation stages compared to those previously created by Lewis *et al.* (2023; Regression A & B), which were fitted and validated to cover data from shores containing lower diversity and more homogenous cover (Figure 8). This was expected for validation stage 1, as this was within-set validation for my BAI model (Figure 8, panels A-D). Critically, my BAI model produced an RMSE of 9.5 when predicting cover using novel shore data, compared to RMSE values of 14.1 and 12.5 from Regressions A & B respectively (Figure 8, panels E-H). This improvement is most likely due to the inclusion of a greater range of naturally occurring diversity and heterogeneity of macroalgal forests within the high-resolution UAV data used to fit the model. The BAI regression model's ability to predict canopy-forming brown macroalgae within +/-10% from satellite imagery is a major step in increasing the scale of macroalgae surveys, where previous efforts to utilise satellite imagery for surveying intertidal macroalgae were precluded by the coarse resolution of open-access multispectral satellite imagery (Brodie et al., 2007; Kotta et al., 2018; Rossiter et al., 2020).

Error in BAI regression techniques

Of the two previously created models' Regression B performed better compared to Regression A, with Regression B producing RMSE values closer to those from my BAI model (Figure 8). However, Lewis *et al.* (2023) found Regression A produced more accurate cover estimates when applied to their validation data containing more homogenous macroalgae cover. Moreover, during novel shore validation, Port Wrinkle contained pixels with up to 25% total cover misidentified by Regression B as containing 0% macroalgal cover. These pixels with up to 25% cover, but lower BAI values relative to pixels in training data were identified to be caused by the presence of low albedo rock decreasing NIR reflectance and therefore producing BAI values outside the model's fitted range (Figure 8 H). A similar effect was also observed at the upper limit of Regression A which is likely due to the high NIR reflectance of large *Ascophyllum nodosum* individuals at Boulmer (Figure 8 G). Variables such as rock albedo and variation of individual macroalgal species reflectivity may weaken the relationship between S2A BAI values and total macroalgal cover. This could again be a symptom of model overfitting to training data, especially in the upper and lower limits of the BAI regression models as BAI values outside of the range of fitted data could not be confidently converted to cover predictions.

32

Therefore, caution is required during the wholesale application of a single BAI regression model, as the performance of regression techniques may not be as consistent on shorelines containing greater variation in environmental variables and macroalgal species compared to those used here, or shores containing novel macroalgal species, rock types or under-canopy communities, that could affect the relationship between BAI values and percentage cover. Further validation imagery from shores containing such differences in characteristics compared to the model's training data is required to test the applicability of BAI regression methods when expanding the application spatially or temporally, where such increased variation of spectral characteristics is likely to be more pronounced.

Application of techniques

The success of using open-access satellite imagery, despite its relatively coarse resolution compared to commercial alternatives, increases the scope of the remote sensing of macroalgal forests to larger spatial scales. The ability to measure macroalgal extents over greater areas could enable the upscaling of efforts to identify the environmental drivers underpinning macroalgal forest abundances and the ecosystem functioning of these habitats across local coastlines or entire regions. Moreover, open-access repositories hold years of captured images for temporal analysis of macroalgae forest spatial extents. Such extensive datasets could be used to monitor long-term fluctuations of ecosystem functionality, such as creating a time series of macroalgal forest's carbon sequestration rather than analysing single points in time (Lewis et al., 2023). Furthermore, temporal imagery could be used to monitor responses to anthropogenic degradation of coastal habitats, from small-scale pollution events to species range shifts in response to climate change (Yesson et al., 2015). While BAI regressions can confidently provide total cover estimates for brown canopy-forming macroalgae, the performance of random forest classifiers here provides cautious optimism for the ability of machine learning techniques to map more specific functional groups within brown macroalgae from satellite imagery. Future efforts to incorporate intra-species variation in reflectivity and increase the quality of training imagery, by capturing more areas of known homogenous class cover, may allow random forests or other machine learning classifiers to create a more universally applicable model to predict macroalgae forest spatial extents. If successful, remotely mapping functional groups could upscale the assessment of relationships between species distributions and environmental conditions to larger areas containing greater levels of environmental variability. By assessing entire regions of coastline, future research could avoid generalisations from patterns observed in small-scale plots. These techniques could then be used to enhance the evaluation of biodiversity's role in maintaining ecosystem functionality in the context of intertidal macroalgal forests, which could then be applied to other important habitats for restoration. Understanding and integrating biodiversity, in addition to simple abundance measures,

could improve the effectiveness of various projects, such as habitat restoration and potential nature-based solutions to climate change.

Conclusion

Random forest classifiers were able to predict intertidal macroalgae functional group cover from open-source satellite multispectral imagery but require the incorporation of intra-species variability in reflectance to improve the accuracy of novel shore estimates. However, if random forest models can be improved, they could better incorporate factors causing variations in spectral reflectance, like individual species reflectivity, and provide a reliable predictive model with greater detail regarding macroalgae community composition. Currently, because of the reduced accuracy of random forest predictions of functional group cover on novel shores, BAI models provided comparatively more robust estimates of total brown canopy cover when fitted to data containing a range of heterogeneity and diversity found naturally occurring within intertidal macroalgal forests. However, the application of a single BAI regression model requires caution as estimates are susceptible to variables that affect green or near-infra-red reflectance such as rock albedo or differences in macroalgae species reflectivity.

References

Balata, D., Piazzi, L., & Rindi, F. (2011). Testing a new classification of morphological functional groups of marine macroalgae for the detection of responses to stress. *Marine Biology*, *158*(11). https://doi.org/10.1007/s00227-011-1747-y

Bayley, D. T. I., Brickle, P., Brewin, P. E., Golding, N., & Pelembe, T. (2021). Valuation of kelp forest ecosystem services in the falkland islands: A case study integrating blue carbon sequestration potential. *One Ecosystem*, *6*. https://doi.org/10.3897/oneeco.6.e62811

Belgiu, M., & Drăguţ, L. (2016b). Random forest in remote sensing: A review of applications and future directions. *ISPRS Journal of Photogrammetry and Remote Sensing*, *114*, 24–31.

Bell, T. W., Okin, G. S., Cavanaugh, K. C., & Hochberg, E. J. (2020). Impact of water characteristics on the discrimination of benthic cover in and around coral reefs from imaging spectrometer data. *Remote Sensing of Environment*, *239*. https://doi.org/10.1016/j.rse.2019.111631

Bertocci, I., Araújo, R., Oliveira, P., & Sousa-Pinto, I. (2015). Potential effects of kelp species on local fisheries. *Journal of Applied Ecology*, *52*(5), 1216–1226. https://doi.org/10.1111/1365-2664.12483

Brodie, J., Ash, L. V., Tittley, I., & Yesson, C. (2018). A comparison of multispectral aerial and satellite imagery for mapping intertidal seaweed communities. *Aquatic Conservation: Marine and Freshwater Ecosystems*, *28*(4). https://doi.org/10.1002/aqc.2905

Brodie, J., Maggs, C. A., & John, D. M. (2007). *Green Seaweeds of Britain and Ireland*.

Burrows, M. T. (2012). Influences of wave fetch, tidal flow and ocean colour on subtidal rocky communities. *Marine Ecology Progress Series*, *445*. https://doi.org/10.3354/meps09422

Congedo, L. (2021). Semi-Automatic Classification Plugin: A Python tool for the download and processing of remote sensing images in QGIS. In *Journal of Open Source Software* (Vol. 6, Issue 64, p. 3172).

Cui, T. W., Liang, X. J., Gong, J. L., Tong, C., Xiao, Y. F., Liu, R. J., Zhang, X., & Zhang, J. (2018). Assessing and refining the satellite-derived massive green macro-algal coverage in the Yellow Sea with high resolution images. *ISPRS Journal of Photogrammetry and Remote Sensing*, *144*. https://doi.org/10.1016/j.isprsjprs.2018.08.001

D'Archino, R., & Piazzi, L. (2021). Macroalgal assemblages as indicators of the ecological status of marine coastal systems: A review. In *Ecological Indicators* (Vol. 129). https://doi.org/10.1016/j.ecolind.2021.107835

DeFries, R. S., & Chan, J. C. W. (2000). Multiple criteria for evaluating machine learning algorithms for land cover classification from satellite data. *Remote Sensing of Environment*, *74*(3). https://doi.org/10.1016/S0034-4257(00)00142-5

Duarte, C. M., Gattuso, J. P., Hancke, K., Gundersen, H., Filbee-Dexter, K., Pedersen, M. F., Middelburg, J. J., Burrows, M. T., Krumhansl, K. A., Wernberg, T., Moore, P., Pessarrodona, A., Orberg, S. B., Pinto, I. S., Assis, J., Queirós, A. M., Smale, D. A., Bekkby, T., Serrao, E. A., & Krause-Jensen, D. (2022). Global estimates of the extent and production of macroalgal forests. *Global Ecology and Biogeography*, *31*(7), 1422–1439. https://doi.org/10.1111/geb.13515

Dudley, T. L., & D'Antonio, C. M. (1991). The effects of substrate texture, grazing, and disturbance on macroalgal establishment in streams. *Ecology*, *72*(1). https://doi.org/10.2307/1938923

Edgar, G. J., & Moore, P. G. (1986). Macro-algae as habitats for motile macrofauna. In *Monografias Biologicas*. *Simposio Internacional. Usos Funciones Ecologicas de las Algas Marinas Bentonicas* (pp. 255–277).

Finger, D. J. I., McPherson, M. L., Houskeeper, H. F., & Kudela, R. M. (2021). Mapping bull kelp canopy in northern California using Landsat to enable long-term monitoring. *Remote Sensing of Environment*, *254*. https://doi.org/10.1016/j.rse.2020.112243

Foody, G. M., Campbell, N. A., Trodd, N. M., & Wood, T. F. (1992). Derivation and applications of probabilistic measures of class membership from the maximum-likelihood classification. *Photogrammetric Engineering & Remote Sensing*, *58*(9).

Greenhill, L., Sundnes, F., & Karlsson, M. (2021). Towards sustainable management of kelp forests: An analysis of adaptive governance in developing regimes for wild kelp harvesting in Scotland and Norway. *Ocean and Coastal Management*, *212*(May), 105816. https://doi.org/10.1016/j.ocecoaman.2021.105816

Hamilton, S. L., Bell, T. W., Watson, J. R., Grorud-Colvert, K. A., & Menge, B. A. (2020). Remote sensing: generation of long-term kelp bed data sets for evaluation of impacts of climatic variation. *Ecology*, *101*(7). https://doi.org/10.1002/ecy.3031

Hawkins, S. J., Pack, K. E., Hyder, K., Benedetti-Cecchi, L., & Jenkins, S. R. (2020). Rocky shores as tractable test systems for experimental ecology. *Journal of the Marine Biological Association of the United Kingdom*, *100*(7), 1017–1041.

Hawkins, S. J., Moore, P., Burrows, M., Poloczanska, E., Mieszkowska, N., Herbert, R., Jenkins, S., Thompson, R., Genner, M., & Southward, A. (2008). Complex interactions in a rapidly changing world: responses of rocky shore communities to recent climate change. *Climate Research*, *37*, 123–133. https://doi.org/10.3354/cr00768

Hu, C. (2009). A novel ocean color index to detect floating algae in the global oceans. *Remote Sensing of Environment, 113*(10). https://doi.org/10.1016/j.rse.2009.05.012

Juanes, J. a., Guinda, X., Puente, a., & Revilla, J. a. (2008). Macroalgae, a suitable indicator of the ecological status of coastal rocky communities in the NE Atlantic. *Ecological Indicators*, *8*(4), 351–359. https://doi.org/10.1016/j.ecolind.2007.04.005

Kotta, J., Valdivia, N., Kutser, T., Toming, K., Rätsep, M., & Orav-Kotta, H. (2018). Predicting the cover and richness of intertidal macroalgae in remote areas: a case study in the Antarctic Peninsula. *Ecology and Evolution*, *8*(17), 9086–9094.

Krumhansl, K. A., & Scheibling, R. E. (2011). Detrital production in Nova Scotian kelp beds: Patterns and processes. *Marine Ecology Progress Series*, *421*. https://doi.org/10.3354/meps08905

Lamy, T., Koenigs, C., Holbrook, S. J., Miller, R. J., Stier, A. C., & Reed, D. C. (2020). Foundation species promote community stability by increasing diversity in a giant kelp forest. *Ecology*, *101*(5). https://doi.org/10.1002/ecy.2987

Lewis, P. H., Roberts, B. P., Moore, P. J., Pike, S., Scarth, A., Medcalf, K., & Cameron, I. (2023). Combining unmanned aerial vehicles and satellite imagery to quantify areal extent of intertidal brown canopy-forming macroalgae. *Remote Sensing in Ecology and Conservation*.

Malthus, T. J., & George, D. G. (1997). Airborne remote sensing of macrophytes in Cefni Reservoir, Anglesey, UK. *Aquatic Botany*, *58*(3–4). https://doi.org/10.1016/S0304-3770(97)00043-0

Metzger, J. R., Konar, B., & Edwards, M. S. (2019). Assessing a macroalgal foundation species: community variation with shifting algal assemblages. *Marine Biology*, *166*(12). https://doi.org/10.1007/s00227-019-3606-1

Miloslavich, P., Bax, N. J., Simmons, S. E., Klein, E., Appeltans, W., Aburto-Oropeza, O., Andersen Garcia, M., Batten, S. D., Benedetti-Cecchi, L., Checkley, D. M., Chiba, S., Duffy, J. E., Dunn, D. C., Fischer, A., Gunn, J., Kudela, R., Marsac, F., Muller-Karger, F. E., Obura, D., & Shin, Y. J. (2018). Essential ocean variables for global sustained observations of biodiversity and ecosystem changes. *Global Change Biology*, *24*(6). https://doi.org/10.1111/gcb.14108

Mora-Soto, A., Palacios, M., Macaya, E. C., Gómez, I., Huovinen, P., Pérez-Matus, A., Young, M., Golding, N., Toro, M., Yaqub, M., & Macias-Fauria, M. (2020). A high-resolution global map of giant kelp (Macrocystis pyrifera) forests and intertidal green algae (Ulvophyceae) with sentinel-2 imagery. *Remote Sensing*, *12*(4), 1–20. https://doi.org/10.3390/rs12040694

Muth, A. F. (2012). Effects of Zoospore Aggregation and Substrate Rugosity on Kelp Recruitment Success. *Journal of Phycology*, *48*(6). https://doi.org/10.1111/j.1529-8817.2012.01211.x

Norderhaug, K. M., Filbee-Dexter, K., Freitas, C., Birkely, S. R., Christensen, L., Mellerud, I., Thormar, J., Van Son, T., Moy, F., Alonso, M. V., & Steen, H. (2020). Ecosystem-level effects of large-scale disturbance in kelp forests. *Marine Ecology Progress Series*, *656*, 163–180. https://doi.org/10.3354/meps13426

Orlando-Bonaca, M., Pitacco, V., & Lipej, L. (2021). Loss of canopy-forming algal richness and coverage in the northern Adriatic Sea. *Ecological Indicators*, *125*. https://doi.org/10.1016/j.ecolind.2021.107501

Pal, M. (2005). Random forest classifier for remote sensing classification. *International Journal of Remote Sensing*, *26*(1), 217–222.

Paola, J. D., & Schowengerdt, R. A. (1995). A Detailed Comparison of Backpropagation Neural Network and Maximum-Likelihood Classifiers for Urban Land Use Classification. *IEEE Transactions on Geoscience and Remote Sensing*, *33*(4). https://doi.org/10.1109/36.406684

Pham, T. D., Ha, N. T., Saintilan, N., Skidmore, A., Phan, D. C., Le, N. N., Viet, H. L., Takeuchi, W., & Friess, D. A. (2023). Advances in Earth observation and machine learning for quantifying blue carbon. *Earth-Science Reviews*, 104501.

Pinedo, S., Garcia, M., Satta, M. P., De Torres, M., & Ballesteros, E. (2007). Rocky-shore communities as indicators of water quality: A case study in the Northwestern Mediterranean. *Marine Pollution Bulletin*, *55*(1–6), 126–135.

Purkis, S. J. (2018). Remote sensing tropical coral reefs: The view from above. In *Annual Review of Marine Science* (Vol. 10). https://doi.org/10.1146/annurev-marine-121916-063249

R Core Team. (2023). R Core Team 2023 R: A language and environment for statistical computing. R foundation for statistical computing. https://www.R-project.org/. *R Foundation for Statistical Computing*.

Rossiter, T., Furey, T., McCarthy, T., & Stengel, D. B. (2020). Application of multiplatform, multispectral remote sensors for mapping intertidal macroalgae: A comparative approach. *Aquatic Conservation: Marine and Freshwater Ecosystems*, *30*(8), 1595–1612.

Schrofner-Brunner, B., Hagan, J. G., Cappelatti, L., Hassellöv, J., Wißmann, M., & Gamfeldt, L. (2023). Macroalgae maintain growth outside their observed distributions: Implications for biodiversity-ecosystem functioning at landscape scales. *Journal of Ecology*.

Shivakumar, B. R., & Rajashekararadhya, S. V. (2018). Investigation on land cover mapping capability of maximum likelihood classifier: A case study on North Canara, India. *Procedia Computer Science*, *143*. https://doi.org/10.1016/j.procs.2018.10.434

Siddiqui, M. D., & Zaidi, A. Z. (2023). Spectral indices for enhancing aquatic vegetation: a case study of seaweed on the Arabian coast of Pakistan using Worldview-2 data. *International Journal of Remote Sensing*. https://doi.org/10.1080/01431161.2023.2247527

Siddiqui, M. D., Zaidi, A. Z., & Abdullah, M. (2019). Performance evaluation of newly proposed seaweed enhancing index (SEI). *Remote Sensing, 11*(12). https://doi.org/10.3390/rs11121434

Teagle, H., Hawkins, S. J., Moore, P. J., & Smale, D. A. (2017). The role of kelp species as biogenic habitat formers in coastal marine ecosystems. In *Journal of Experimental Marine Biology and Ecology* (Vol. 492). https://doi.org/10.1016/j.jembe.2017.01.017

Thornber, C. S., Jones, E., & Thomsen, M. S. (2016). Epibiont-Marine Macrophyte Assemblages. In *Marine Macrophytes as Foundation Species*.

Timmer, B., Reshitnyk, L., Hessing-Lewis, M., Juanes, F., Gendall, L., & Costa, M. (2024). Capturing accurate kelp canopy extent: integrating tides, currents, and

species-level morphology in kelp remote sensing. *Frontiers in Environmental Science*, *12*.

Uhl, F., Oppelt, N., & Bartsch, I. (2013). Spectral mixture of intertidal marine macroalgae around the island of Helgoland (Germany, North Sea). *Aquatic Botany*, *111*. https://doi.org/10.1016/j.aquabot.2013.06.001

Underwood, A. J. (2000). Experimental ecology of rocky intertidal habitats: what are we learning? *Journal of Experimental Marine Biology and Ecology*, *250*(1–2), 51–76. http://www.sciencedirect.com/science/article/pii/S0022098100001799

Underwood, A. J., & Jernakoff, P. (1984). The effects of tidal height, wave-exposure, seasonality and rock-pools on grazing and the distribution of intertidal macroalgae in New South Wales. *Journal of Experimental Marine Biology and Ecology*, *75*(1). https://doi.org/10.1016/0022-0981(84)90024-8

Veettil, B. K., Ward, R. D., Lima, M. D. A. C., Stankovic, M., Hoai, P. N., & Quang, N. X. (2020). Opportunities for seagrass research derived from remote sensing: A review of current methods. In *Ecological Indicators* (Vol. 117). https://doi.org/10.1016/j.ecolind.2020.106560

Vondolia, G. K., Chen, W., Armstrong, C. W., & Norling, M. D. (2020). Bioeconomic Modelling of Coastal Cod and Kelp Forest Interactions: Co-benefits of Habitat Services, Fisheries and Carbon Sinks. *Environmental and Resource Economics*, *75*(1), 25–48. https://doi.org/10.1007/s10640-019-00387-y

Wang, L., Jia, M., Yin, D., & Tian, J. (2019). A review of remote sensing for mangrove forests: 1956–2018. *Remote Sensing of Environment*, *231*. https://doi.org/10.1016/j.rse.2019.111223

Wang, M., & Hu, C. (2021). Satellite remote sensing of pelagic Sargassum macroalgae: The power of high resolution and deep learning. *Remote Sensing of Environment*, *264*. https://doi.org/10.1016/j.rse.2021.112631

Weiskopf, S. R., Myers, B. J. E., Arce-Plata, M. I., Blanchard, J. L., Ferrier, S., Fulton, E. A., Harfoot, M., Isbell, F., Johnson, J. A., & Mori, A. S. (2022). A conceptual framework to integrate biodiversity, ecosystem function, and ecosystem service models. *BioScience*, *72*(11), 1062–1073.

Wing, S. R., Durante, L. M., Connolly, A. J., Sabadel, A. J. M., & Wing, L. C. (2022). Overexploitation and decline in kelp forests inflate the bioenergetic costs of fisheries. *Global Ecology and Biogeography*, *31*(4), 621–635. https://doi.org/10.1111/geb.13448

Yesson, C., Bush, L. E., Davies, A. J., Maggs, C. A., & Brodie, J. (2015). Large brown seaweeds of the british isles: Evidence of changes in abundance over four decades. *Estuarine, Coastal and Shelf Science*, *155*. https://doi.org/10.1016/j.ecss.2015.01.008